Silicon-Containing Trifunctional and Tetrafunctional Cyanate Esters: Synthesis, Cure Kinetics, and Network Properties

Andrew J. Guenthner,[1] Vandana Vij,[2] Timothy S. Haddad,[2] Josiah T. Reams,[2] Kevin R. Lamison,[2] Christopher M. Sahagun,[3] Sean M. Ramirez,[2] Gregory R. Yandek,[1] Suresh C. Suri,[1] Joseph M. Mabry[1]

[1]Aerospace Systems Directorate, Air Force Research Laboratory, Edwards AFB, California 93524
[2]ERC Incorporated, Air Force Research Laboratory, Edwards AFB, California 93524
[3]National Research Council/Air Force Research Laboratory, Edwards AFB, California 93524
Correspondence to: A. J. Guenthner (E-mail: andrew.guenthner@edwards.af.mil)

Received 25 October 2013; accepted 22 November 2013; published online 18 December 2013
DOI: 10.1002/pola.27052

ABSTRACT: The synthesis and physical properties of new silicon-containing polyfunctional cyanate ester monomers methyl[tris(4-cyanatophenyl)]silane and tetrakis(4-cyanatophenyl)silane, as well as polycyanurate networks formed from these monomers are reported. The higher crosslinking functionality compared to di(cyanate ester) monomers enables much higher ultimate glass transition temperatures to be obtained as a result of thermal cyclotrimerization. The ability to reach complete conversion is greatly enhanced by cocure of the new monomers with di(cyanate ester) monomers such as 1,1-bis(4-cyanatophenyl)ethane. The presence of silicon in these polycyanurate networks imparts improved resistance to rapid oxidation at elevated temperatures, resulting in char yields as high as 70% under nitrogen and 56% in air in the best-performing networks. The water uptake in the silicon-containing networks examined is 4–6 wt % after 96 h of immersion at 85 °C, considerably higher than both carbon-containing and/or di(cyanate ester) analogs. © 2013 Wiley Periodicals, Inc. J. Polym. Sci., Part A: Polym. Chem. **2014**, *52*, 767–779

KEYWORDS: curing of polymers; cyanate ester; differential scanning calorimetry (DSC); high performance polymers; polycyanurate; silane; thermosets

INTRODUCTION Polycyanurate networks formed from the cyclotrimerization of cyanate ester monomers have proven to be an especially useful class of thermosetting material, with numerous high-performance applications in the microelectronics and aerospace industries.[1–4] Some of the more interesting example applications include magnet casing for nuclear fusion reactors[5,6] and the Large Hadron Collider,[7] brush seals for turbine engines,[8,9] and spacecraft structures such as frameworks for telescope mirrors,[10] and solar panel supports.[11] In many applications, protection against oxidation during short-term exposure to temperatures at or above 500 °C is highly desirable. Unfortunately, the onset of thermochemical degradation in the triazine crosslinks of cyanurate networks occurs well below 500 °C,[12] thus thermooxidative protection must be provided by the incorporation of more stable materials.

A strategy used to provide thermooxidative protection in cyanurate polymer networks that has been explored through much recent investigation is the incorporation of silicon or siloxy moieties in the form of monomers and cocuratives,[13–21] blends and modifiers,[22–24] silica nanoparticles,[25–34] clay nanoplatelets,[35–47] or other silicon-containing nanostructures[48–53] including oligomeric silsesquioxanes.[54–66] While the addition of silicon in fully oxidized form (i.e., as SiO_2) can provide an in-place barrier to oxygen permeation, the use of unoxidized organosilicon moieties or partly oxidized silicates allows for the *in situ* generation of a protective barrier during high-temperature oxidation or exposure to energetic forms of oxygen (such as atomic oxygen in low Earth orbit).[66–68] Such *in situ* generation from the bulk has the advantage of spontaneous regeneration in the event that a protective layer is breached or damaged during further exposure. Furthermore, the incorporation of silicon at the molecular level by the use of organosilicon small-molecule monomers (either as single component substitutes or as cocuratives) can preserve desirable processing characteristics such as a low viscosity in the uncured state.

To date, there have been several reports relating to organosilicon monomers for epoxy,[13,14,69–73] benzoxazine,[74] and bismaleimide[18,75–77] thermosetting networks. In cyanate esters,

Additional Supporting Information may be found in the online version of this article.

a silicon-containing analog (named SiMCy) to the well-known dicyanate ester of bisphenol A (BADCy) was first synthesized by Wright et al. in 2003.[20] Compared to BADCy, SiMCy exhibited improved thermooxidative resistance at high temperatures along with lower water uptake, and improved processing and cure characteristics.[19] Two cyanate ester organosilane monomers have also been described recently for use in the formation of microporous structures.[15]

Though the incorporation of silicon at the molecular level in thermosetting polymers offers improved thermooxidative resistance, it can have negative effects on other aspects of performance. Because the carbon–silicon bond is in general longer and more flexible than a corresponding carbon–carbon bond, the molecular segments of networks containing such bonds are more flexible, resulting in a lower glass transition temperature at full cure, when silicon is incorporated into the network.[17,19] Approaches to the molecular level incorporation of silicon that enable the networks to retain high glass transition temperatures at full cure are therefore of considerable interest. To date, however, there has been very little work devoted to demonstrating means of incorporating molecular-level silicon in a manner that facilitates the retention of high glass transition temperatures at full cure.

In this article, we report the synthesis, cure kinetics, and network properties of trifunctional and tetrafunctional silicon-containing cyanate esters in which the silicon serves as a network junction point after cure. It has been shown that the incorporation of network junctions, whether they arise from crosslinks or from branch points in tri- (or higher) functional monomers with functional end groups, provide for an increased glass transition temperature at full cure in thermosetting composite resins.[78] By incorporating silicon into trifunctional and tetrafunctional monomers in such a way as to create a network junction coincident with each incorporated silicon atom, we show that networks are obtained that exhibit glass transition temperatures higher than those of the corresponding networks formed from difunctional cyanate esters without silicon. We further show that these advantages are retained when the silicon-containing monomers are cocured with di(cyanate ester)s such as Primaset® 1,1-bis(4-cyanatophenyl)ethane (LECy) in order to achieve complete conversion to cyanurates. These networks thus offer both high glass transition temperatures as well as increased thermooxidative stability while retaining good processing characteristics.

EXPERIMENTAL

General Considerations

Primaset® BADCy and Primaset® LECy were purchased from Lonza and used as received. SiMCy, that is, bis(4-cyanatophenyl)dimethylsilane, was synthesized according to a previously published procedure.[17] ESR-255, that is, tris(4-cyanatophenyl)ethane, was synthesized according to a previously published procedure[79] by Dr Matthew Davis at the Naval Air Warfare Center, Weapons Division, China Lake, CA, and used as received. Tetrahydrofuran (THF), diethyl ether (ether), chloroform, hexane, and toluene were dried by passage through columns of activated alumina under a nitrogen atmosphere and then degassed before use. Anhydrous dichloromethane and acetone were purchased from Aldrich and used as received. Methyltrichlorosilane and tetrachlorosilane were purchased from Gelest and distilled before use. Triethylamine was purchased from Aldrich Chemical and distilled before use. 4-Benzyloxybromobenzene was obtained from Aldrich and recrystallized from ether before use. Cyanogen bromide, *n*-butyllithium, nonylphenol, and 10% palladium on carbon (wet, Degussa type) were obtained from Aldrich Chemical and used as received. Copper(II) acetylacetonate was purchased from ROC/RIC and used as received. All manipulations of compounds and solvents for the preparation of compounds (**1**)–(**6**) were carried out using standard Schlenk line techniques. Hydrogenation was done using a Parr Hydrogenator equipped with pressure safe vessels and Viton® seals. Selected cyanate ester samples were purified using a W-Prep2XY Yamazen chromatographic column.

Preparation of Methyl[tris(4-benzyloxyphenyl)]silane (1)

A chilled (−78 °C) THF (400 mL) solution of 4-bromophenyl benzyl ether (20.00 g, 76.0 mmol was treated with 2.5M *n*-BuLi (30.4 mL, 76 mmol) and allowed to react with stirring for 2 h at −78 °C. This mixture, now heterogeneous, was treated with slow addition of methyltrichlorosilane (3.787 g, 25.33 mmol, diluted with THF) and the cooling bath removed. The mixture was allowed to react with stirring overnight and the solvents were removed under reduced pressure. Chloroform (300 mL) was added, and the mixture was stirred for additional hour. This was filtered to remove LiCl salt, and the solvent from the filtrate was removed under reduced pressure on a rotary evaporator. The off-white crude product was precipitated into methanol (400 mL). This was stirred overnight, filtered, and dried under nitrogen to afford **1** as a white solid (13 g, 87% yield).

^{1}H NMR (acetone-d_6) δ: 7.48–7.32 (m, 21H), 7.03 (d, $J = 8$ Hz, 6H), 5.12 (s, 6H), 0.75 (s, 3H). ^{13}C NMR (acetone-d_6) δ: 160.94 (C4), 138.32 (C6), 137.47 (C2), 136.86 (C1), 129.35 (C8), 128.70 (C9), 128.50 (C7), 115.38 (C3), 70.23 (C5), −2.66 (C10, SiCH$_3$). ^{29}Si NMR (acetone-d_6) δ: −12.32 (s).

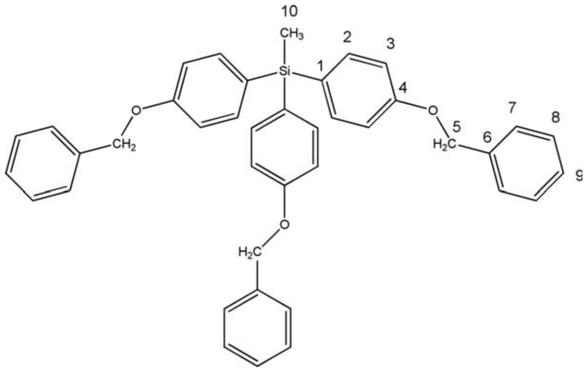

Combustion analysis calculated (Found): % C, 81.04 (80.77); % H, 6.12 (6.13).

Preparation of Methyl[tris(4-hydroxyphenyl)]silane (2)

A THF (200 mL) solution containing **1** (10.00 g, 16.87 mmol) and 10 wt % palladium on carbon (400 mg), was placed in a 1000-mL pressure-safe vessel equipped with Viton® seals and connected to a hydrogenator. This was pressurized with hydrogen (35 psi) and allowed to react with stirring for 48 h. The catalyst was removed by filtration through Celite, and the solvent was removed under reduced pressure to afford 4.60 g (85% yield) of **2**, as an off-white solid. For purification, compound **2** was dissolved in THF and precipitated out in hexane. The white product was filtered, washed with ether, and dried under dynamic vacuum.

^{1}H NMR (acetone-d_6) δ: 8.47 (s, 3H), 7.34 (d, $J = 8$ Hz, 6H), 6.87 (d, $J = 8$ Hz, 6H), 0.70 (s, 3H). ^{13}C NMR (acetone-d_6) δ: 159.43 (C4), 137.52 (C2), 127.37 (C1), 115.92 (C3), −2.51 (C5, $SiCH_3$). ^{29}Si NMR (acetone-d_6) δ: −12.57 (s). Combustion analysis calculated (Found): % C, 70.78 (70.35); % H, 5.63 (5.69).

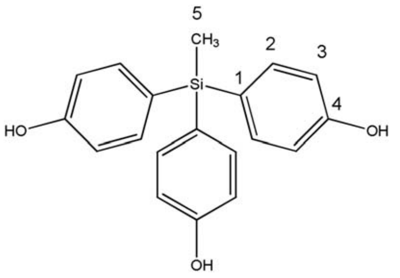

Preparation of Methyl[tris(4-cyanatophenyl)]silane (3)

A chilled (−20 °C) ether (200 mL) solution containing methyl[tris(4-hydroxyphenyl)]silane, **2**, (4.0 g, 12.41 mmol) and cyanogen bromide (4.88 g, 46.53 mmol) was treated with triethylamine (4.71 g, 46.53 mmol) in a drop-wise manner. This mixture was allowed to react for 2 h with stirring at −20 °C. Diethyl ether (500 mL) was added to the reaction mixture and stirred overnight. The mixture was filtered to remove the hydrobromide salt, and the organic layer was washed with (2 × 100 mL) DI water, followed by a brine wash and then dried over $MgSO_4$. The solvents were removed under reduced pressure, and crude product (3.2 g, 65% yield) was precipitated out from ether to afford 2.9 g (59% yield) of **3** as white crystalline solid (mp 118 °C). Some batches of cyanate ester **3** were further purified by flash chromatography using silica–gel (40 μm, 60 Å) universal column size M (20 ID × 80-mm packed length) with a dichloromethane mobile phase.

^{1}H NMR (acetone-d_6) δ: 7.74 (d, $J = 9$ Hz, 6H), 7.48 (d, $J = 9$ Hz, 6H), 0.98 (s, 3H). ^{13}C NMR (acetone-d_6) δ: 154.48 (C4), 137.37 (C2), 134.11 (C1), 115.13 (C3), 108.20 (C6, OCN), −4.43 (C5, $SiCH_3$). ^{29}Si NMR (acetone-d_6) δ: −10.51 (s). Combustion analysis Calculated (Found): % C, 66.48 (66.01); % H, 3.80 (3.68); % N, 10.57 (10.68).

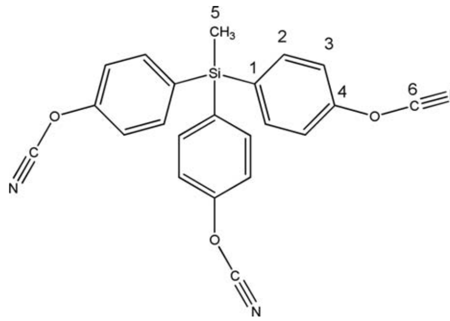

Preparation of Tetrakis(4-benzyloxyphenyl)silane (4)

A chilled (−78 °C) THF (400 mL) solution of 4-bromophenyl benzyl ether (20.00 g, 76.0 mmol was treated with 2.5M *n*-BuLi (30.4 mL, 76 mmol) and allowed to react with stirring for 2 h at −78 °C. This mixture, now heterogeneous, was treated with a slow addition of tetrachlorosilane (3.22 g, 19 mmol, diluted with THF), and the cooling bath removed. The mixture was allowed to reflux at 55 °C with stirring for two nights. The solvents were removed under reduced pressure. Chloroform (300 mL) was added, and the mixture was stirred for additional hour. This was filtered to remove LiCl salt, and the solvent from the filtrate was removed under reduced pressure on a rotary evaporator. The off-white crude product was precipitated into methanol (400 mL). This was stirred overnight, filtered, and dried under nitrogen to afford **4** as a white solid (11 g, 76% yield).

^{1}H NMR ($CDCl_3$) δ: 7.54–7.38 (m, 28H), 7.05 (d, $J = 9$ Hz, 8H), 5.12 (s, 8H). ^{13}C NMR ($CDCl_3$) δ: 160.54 (C4), 137.84 (C2), 136.98 (C6), 128.66 (C8), 128.06 (C9), 127.59 (C7), 126.42 (C1), 114.46 (C3), 69.80 (C5). ^{29}Si NMR ($CDCl_3$) δ: −14.60 (s). Combustion analysis Calculated (Found): % C, 82.07 (81.49); % H, 5.83 (5.90).

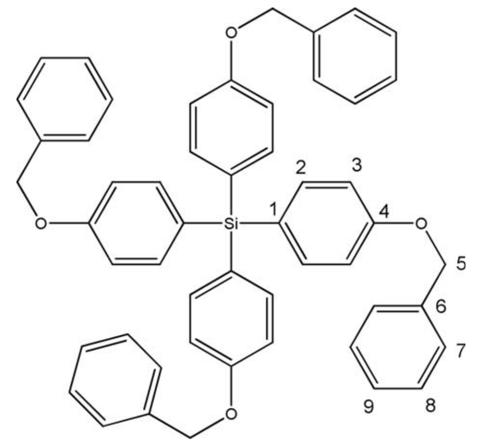

Preparation of Tetrakis(4-hydroxyphenyl)silane (5)

A THF (200 mL) solution containing **4** (10.00 g, 13.14 mmol) and 10 wt % palladium on carbon (400 mg) was placed in a 1000-mL pressure-safe vessel equipped with Viton® seals and connected to a hydrogenator. This was placed under an atmosphere of hydrogen (35 psi) and allowed to react with stirring for 48 h. The catalyst was removed by filtration through Celite, and the solvent was removed under reduced pressure to afford 4.80 g (91% yield) of **5** as an off-white solid. For purification, compound **5** was dissolved in THF and precipitated out in hexane. The white product was filtered, washed with ether, and dried under dynamic vacuum.

^{1}H NMR (acetone-d_6) δ: 8.63 (s, 4H), 7.38 (d, $J = 6$ Hz, 8H), 6.81 (d, $J = 6$ Hz, 8H). ^{13}C NMR (acetone-d_6) δ: 159.54 (C4), 138.59 (C2), 125.98 (C1), 115.92 (C3). ^{29}Si NMR (acetone-d_6) δ: -14.64 (s). Combustion analysis calculated (Found): % C, 71.97 (68.89); % H, 5.03 (5.55).

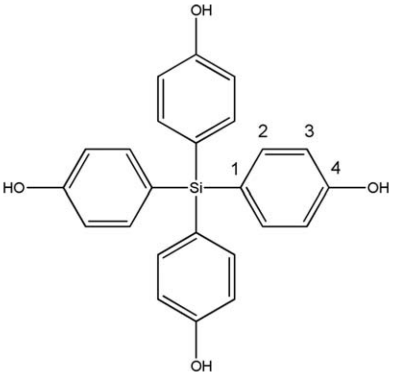

Preparation of Tetrakis(4-cyanatophenyl)silane (6)

A chilled (-20 °C) ether (200 mL) and THF (5 mL) solution containing tetrakis(4-hydroxyphenyl)silane, **5**, (4.0 g, 10 mmol) and cyanogen bromide (5.22 g, 50.mmol) was treated with triethylamine (5.06 g, 50 mmol) in a drop-wise manner. This mixture was allowed to react for 2 h with stirring at -20 °C. Dichloromethane (200 mL) was added to the reaction mixture and stirred for an hour. The mixture was filtered to remove the hydrobromide salt, and the organic layer was washed with (2 × 100 mL) DI water, followed by a brine wash and then dried over $MgSO_4$. The solvents were removed under reduced pressure, and crude product (3.8 g, 76% yield) was precipitated from ether to afford 3.5 g (70% yield) of **6** as white crystalline solid (mp 169 °C).

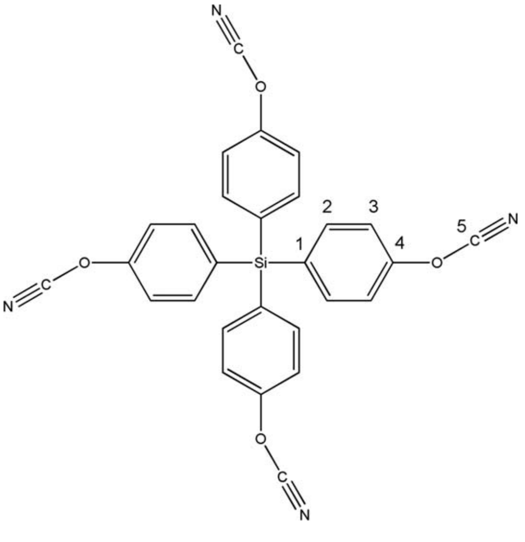

^{1}H NMR (acetone-d_6) δ: 7.77 (d, $J = 8$, 8H), 7.54 (d, $J = 8$, 8H). ^{13}C NMR (acetone-d_6) δ: 155.73 (C4), 139.72 (C2), 132.38 (C1), 116.40 (C3), 109.02 (C5, OCN). ^{29}Si NMR (acetone-d_6) δ: -14.95 (s). Combustion analysis Calculated (Found): % C, 67.19 (67.21); % H, 3.22 (3.27); % N, 11.19 (10.84).

Preparation of Thermally Cured Networks

Cured networks were prepared from the newly synthesized cyanate esters (**3**) and (**6**), blends of (**3**) and (**6**) with the commercial dicyanate ester Primaset® LECy (1,1-bis(4-cyanatophenol)ethane), and three different "control" materials: (1) Primaset® BADCy (2,2-bis(4-cyanatophenyl)propane), (2) SiMCy (bis(4-cyanatophenyl)dimethylsilane), and (3) ESR-255[89] (1,1,1-tris(4-cyanatophenyl)ethane). The properties of SiMCy[16,17,19,20] and ESR-255[79,80] have been described in numerous previous publications. To assess the effects of purity, some batches of (**3**) and SiMCy were purified by passing solutions in dichloromethane through a W-Prep2XY Yamazen flash chromatograph, followed by rotary evaporation.

To mix monomers for cocuring of blended networks, equal weights of each component were weighed out into a vial and then heated to 10–20 °C above the highest melting point of any of the system components and stirred together. An analogous procedure was used for single-component networks except that no stirring was required. Once prepared in a homogeneous, molten state, networks were de-gassed for 30 min under reduced pressure (ca. 300 mmHg), then poured into cylindrical molds measuring 12 mm in diameter × about 3 mm deep composed of silicone rubber. Details of the mold-making procedure have been published elsewhere.[81] The samples were then heated under dry nitrogen to 150 °C for 1 h, followed by 210 °C for 24 h, using ramp rates of 5 K min^{-1}. Once cooled, the samples were de-molded to form homogeneous discs.

Characterization

^{1}H, ^{13}C, and ^{29}Si NMR measurements were performed using a Bruker AC 300 or Bruker 400 MHz instrument. ^{1}H and ^{13}C NMR chemical shifts are reported relative to the deuterated solvent peak (^{1}H, ^{13}C: acetone-d_6, δ 2.05 ppm, δ 29.9 ppm or $CDCl_3$, δ 7.28 ppm, δ 77.23 ppm). ^{29}Si NMR chemical shifts are reported relative to external tetramethylsilane at 0 ppm. Elemental analyses were obtained from Atlantic Microlabs or performed on a Perkin Elmer EA2400 Series II combustion analyzer.

Differential scanning calorimetry (DSC) was carried out on a TA Instruments Q Series 200 instrument under 50 mL min^{-1} dry nitrogen purge. Several different programs were used for analysis. Standard nonisothermal analysis involved heating samples at 10 K min^{-1} to 350 °C, cooling at 10 K min^{-1} to 100 °C, and then reheating to 350 °C at 10 K min^{-1} to establish a baseline. For cure kinetics studies, samples were first heated at 5 K min^{-1} to 130 °C to achieve any required melting, then heated as quickly as possible (~100 K min^{-1}) to the desired isothermal cure temperature and held for 30 min isothermally. Following the isothermal cure, the samples were quenched (~100 K min^{-1} cooling) to 120 °C and then heated to 350 °C at 10 K min^{-1}. The samples were then cooled at 10 K min^{-1} to 100 °C, and the entire procedure was repeated with the cured sample in place to establish a baseline. The details of this procedure, including the method of applying baseline corrections, have been published previously.[80] Cure kinetics were determined using the Kamal model[82] with a variant of Kenny's graphical method;[83] complete details of this procedure have also been published previously.[80]

Thermogravimetric analysis (TGA) was carried out using a TA Instruments Q5000 under 50 mL min^{-1} sample gas purge (dry nitrogen or air), and 10 mL min^{-1} balance gas purge (with gas type matched to the sample). TGA samples were comprised of small chunks of cured discs, and were heated at 10 K min^{-1} to 600 °C. Oscillatory thermomechanical analysis (TMA) was performed using a TA Instruments Q400, with a 50 mL min^{-1} dry nitrogen purge. Cured discs were subjected to a mean compressive force of 0.1 N, oscillating with an amplitude of 0.1 N and a frequency of 0.05 Hz. Samples were preloaded with a 0.2-N force to help achieve good contact with the probe, which consisted of the 5-mm diameter cylindrical "standard" quartz probe supplied by TA Instruments. For "dry" TMA analysis, samples were cycled between 100 and 200 °C twice at 10 K min^{-1} to measure thermal lag (details of this procedure are published elsewhere),[81] then heated to 350 °C at 10 K min^{-1}, cooled to 100 °C at 10 K min^{-1}, and then reheated to 350 °C at 10 K min^{-1}. For "wet" TMA analysis, samples were first heated to 350 °C, then cycled between 100 and 200 °C to measure thermal lag, then reheated to 350 °C, all at 20 K min^{-1}. The procedure for "wet" TMA is designed to minimize drying of the sample before measurement of the glass transition temperature.

Crystal data for compounds (**3**) and (**6**) were collected at $T = 100.0$ (K) using Kusing Bruker 3-circle, SMARTAPEX CCD with c-axis fixed at 54.748, running on SMART V 5.625 program (Bruker AXS: Madison, 2001). Graphite monochromated $\text{Mo}_{\text{K}\alpha}$ ($\lambda = 0.71073$ Å) radiation was employed for data collection and corrected for Lorentz and polarization effects using SAINT V 6.22 program (Bruker AXS: Madison, 2001), and reflection scaling (SADABS program, Bruker AXS: Madison, WI, 2001). Structures were solved by direct methods (SHELXL-97, Bruker AXS: Madison, 2000) and all nonhydrogen atoms refined anisotropically using full-matrix least-squares refinement on F^2. Hydrogen atoms were added at calculated positions when necessary. CDCC 960730 (SiCy-3) and CDCC 960731 (SiCy-4) contain the supplementary crystallographic data for this article. The data can be obtained free of charge from the Cambridge Crystallographic Data Centre via www.ccdc.cam.ac.uk/data_request/cif.

Densities were determined by immersing cured discs in solutions of CaC1_2 and varying the CaCl_2 concentration until neutral buoyancy was achieved. The density of the fluid needed to achieve neutral buoyancy was then determined by weighing 10.00 mL of the fluid in a volumetric flask. Fourier transform infrared spectroscopy (FTIR) was carried out using a Thermo Corporation Nicolet 6700 spectrometer in attenuated total reflectance mode with the ZnSe crystal attachment. A total of 32 scans were completed on these surfaces with a resolution of 4 cm^{-1} to obtain spectra.

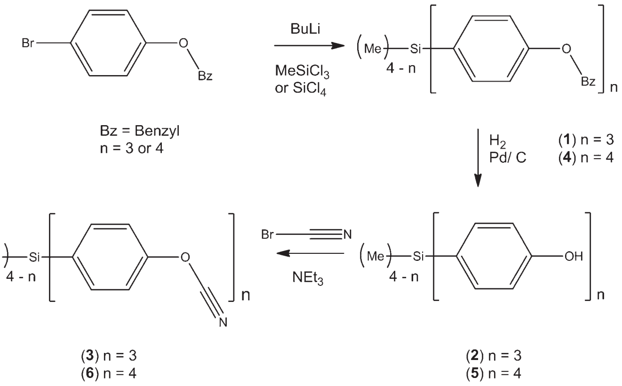

SCHEME 1 Synthesis of new cyanate ester derivatives SiCy-3 (**3**) and SiCy-4 (**6**).

RESULTS AND DISCUSSION

Synthesis of New Monomers (3) and (6)

The new cyanate ester monomers (**3**) and (**6**) were synthesized following the procedures similar to those published for production of SiMCy[17] (See Scheme 1). Lithium-bromo exchange on *p*-bromophenyl benzyl ether with butyllithium produces a nucleophile, which can be used to replace all the chlorides on tetrachlorosilane or methyltrichlorosilane with benzyloxyphenyl groups to produce compounds (**1**) and (**4**). The "protecting" benzyl group is easily removed by low-pressure hydrogenation catalyzed with 10% palladium on carbon to produce phenols (**2**) and (**5**). These phenols react in high yield with cyanogen bromide in the presence of triethylamine to produce the desired cyanate ester monomers (**3**) and (**6**). All six compounds were isolated in high yield and fully characterized by ^{1}H, ^{13}C, and ^{29}Si NMR spectroscopies and combustion analysis. Their spectra are simple and unremarkable with chemical shifts all in the expected regions and ratios. The data are presented in the Experimental section. Additional verification of the structures of (**3**) and (**6**) was provided by X-ray diffraction of single crystals. The resultant structures are shown in Figures 1 and 2. All bond angles and bond lengths are in the expected ranges for such compounds.

Figure 3 provides the structures of all the monomers utilized. ESR-255 is the carbon-containing analog of the silicon-containing tricyanate (**3**). SiMCy is the dicyanate analog of (**3**) in which one cyanate ester functional arm has been replaced by a methyl group, and BADCy is the carbon-containing analog of SiMCy. The carbon-containing analog of (**6**) has been reported previously,[84] but was difficult to cure into a network, thus substantial physical property data are unavailable. Previous work on tricyanate esters has shown that preparing networks comprising 50 wt % of the dicyanate with 50 wt % LECy can result in synergistic improvements in performance.[85] Thus, networks were also prepared from mixtures of equal parts by weight of (**3**) with LECy and (**6**) with LECy, as well as with equal parts of ESR-255 and LECy for comparison. For all investigations, no catalysts were added to the monomers before network formation.

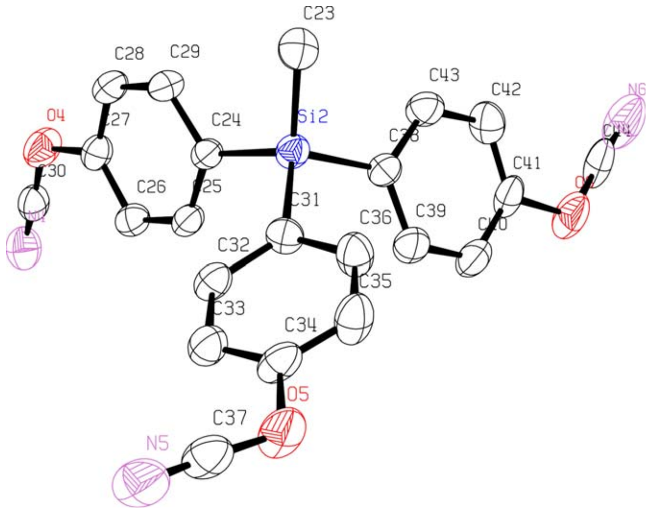

FIGURE 1 ORTEP representation of SiCy-3 (**3**) collected at 100 K. Thermal ellipsoids shown at 50%. Hydrogen atoms omitted for clarity. Black, C; blue, Si, red, O; purple, N. [Color figure can be viewed in the online issue, which is available at wileyonlinelibrary.com.]

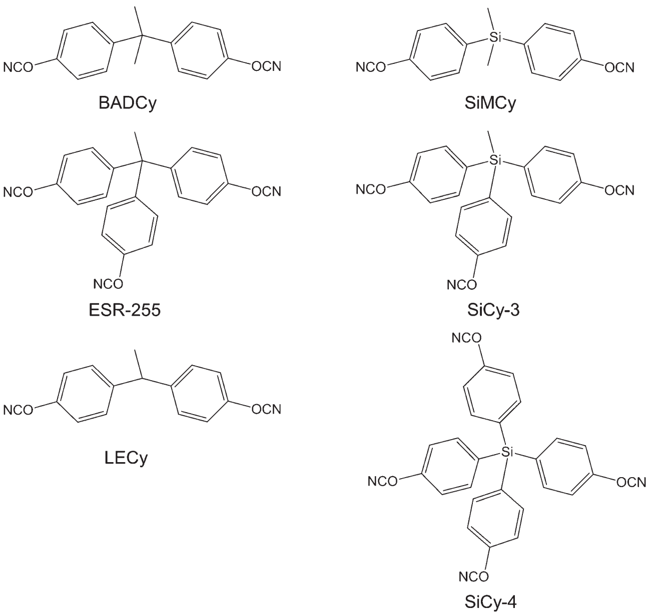

FIGURE 3 Chemical structure of monomers utilized for comparative studies.

Cure Characteristics of Monomers (3) and (6)

The nonisothermal DSC scan, shown in Figure 4, for SiCy-3 (**3**) after purification by chromatography, is typical for highly pure cyanate ester monomers, with recrystallization of the supercooled melt at 50–100 °C followed by melting at 118 °C, a very wide processing window, and cyclotrimerization onset near 300 °C. Both the melting temperature and enthalpy are very similar to that of 1,1,1-tris(4-cyanatophenyl)ethane (known as ESR-255), the carbon-containing analog of SiCy-3. (A full set of comparative nonisothermal DSC data for all monomers studied is provided in Supporting Information Section S2.) The "L"-shaped exotherm associated with cure is indicative of incomplete conversion, as further indicated by an enthalpy of cyclotrimerization of 94 ± 4 kJ per cyanate molar equivalent, versus an expected value of around 110 kJ equiv^{-1}. In fact, the enthalpies of cyclotrimerization for SiCy-3 and ESR-255 are not significantly different when measured by the same nonisothermal DSC protocol, indicating that the more flexible C–Si linkages are ineffective at relieving the steric constraints that prevent complete cyclotrimerization of these tricyanate monomers. An "L"-shaped exotherm with incomplete conversion is also a good indication that, due to vitrification, a sample is in the glassy state at the end of the DSC scan. For SiCy-3, then, the glass transition temperature (T_G) exceeds 350 °C even for the

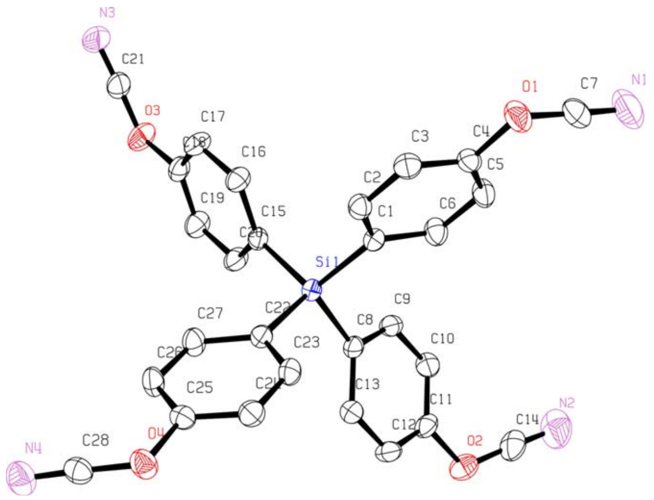

FIGURE 2 ORTEP representation of SiCy-4 (**6**) collected at 100 K. Thermal ellipsoids shown at 50%. Hydrogen atoms omitted for clarity. Black, C; blue, Si, red, O; purple, N. [Color figure can be viewed in the online issue, which is available at wileyonlinelibrary.com.]

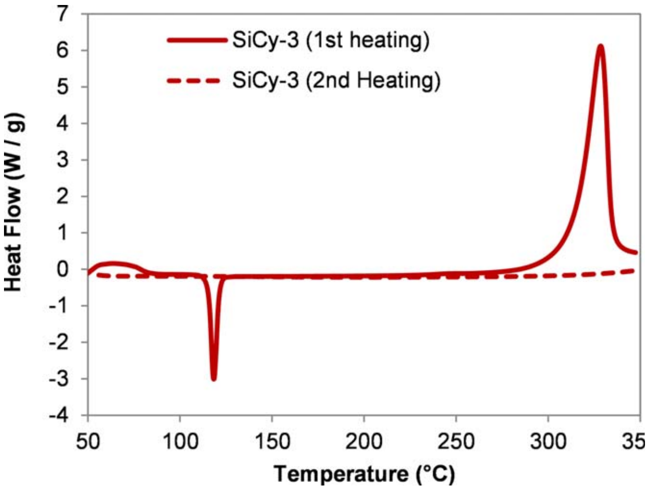

FIGURE 4 Nonisothermal DSC of SiCy-3 (**3**). [Color figure can be viewed in the online issue, which is available at wileyonlinelibrary.com.]

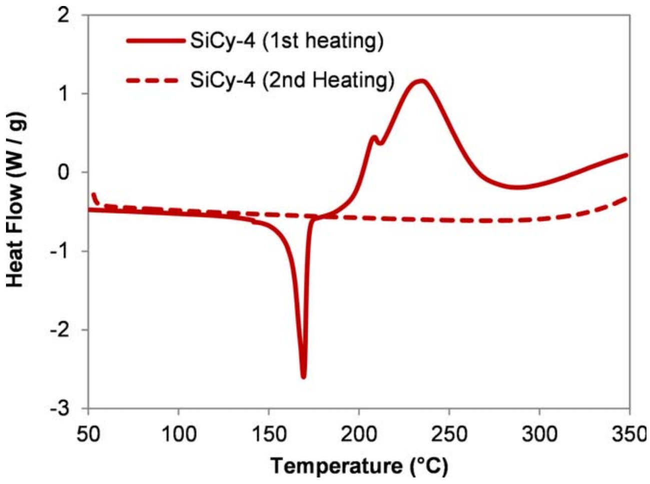

FIGURE 5 Nonisothermal DSC of SiCy-4 (**6**). [Color figure can be viewed in the online issue, which is available at wileyonlinelibrary.com.]

incompletely cured network. Thermochemical degradation of SiCy-3 networks begins at 350–400 °C according to TGA data (see Fig. 12). Thus, although these networks cannot be fully cyclotrimerized, sufficient conversion can be attained to prevent the significant mechanical softening associated with the T_G before the onset of thermochemical degradation. In other words, chemical, rather than mechanical, stability considerations will limit the high-temperature performance of these networks in many situations.

The nonisothermal DSC of SiCy-4 (Fig. 5) indicates that similar steric constraints on cyclotrimerization exist for the tetracyanate analog of SiCy-3. Furthermore, the high melting point precludes many low-cost processing operations. Owing to its low potential for use, further work with the neat nmonomer, including purification by chromatography, was not attempted, although promising results were obtained when cocured with Primaset® LECy (*vide infra*). As a result of the lower purity, the cyclotrimerization exotherm in SiCy-4 (Fig. 5) is shifted to much lower temperatures compared to SiCy-3 (Fig. 4), resulting in a very prominent "L"-shaped exotherm. The total enthalpy of cyclotrimerization (at 96 ± 10 kJ equiv^{-1}) is not significantly different from SiCy-3.

Isothermal DSC analysis of the cyclotrimerization of SiCy-3 produced a pattern of conversion as a function of time and temperature similar to most cyanate ester monomers, as seen in Figure 6. The cure kinetics up to 50% conversion were described well by the Kamal model[82] using analysis procedures that have been described in detail elsewhere.[80] (A complete listing of model parameter values and conversion as a function of time and temperature graphs for SiCy-3 and its many analogs, including analysis of batch to batch reproducibility and effects of purity level, are provided in Supporting Information Section S3.) Arrhenius analysis of the cyclotrimerization of SiCy-3 after purification by chromatography (Fig. 7) resulted in an estimated activation energy of 115 ± 1 kJ mol^{-1}. Note that this uncertainty estimate reflects only the precision of the Arrhenius model fit to the data. When two separate batches of SiCy-3 were analyzed, the computed activation energy differed by about 7% (see Supporting Information Fig. S23). Thus, the value of 107 ± 1 kJ mol^{-1} for ESR-255 reported previously[80] does not reflect a significant difference. In neither the tricyanates nor their dicyanate analogs (see Supporting Information Section S3) were any significant difference in activation energy observed when considering the effect of substitution of Si for C in highly pure samples. Note that the absolute conversion rates observed did vary significantly among monomers and batches with differing purities (but not among highly purified batches of the same monomer), a reflection of the fact that the cyclotrimerization of cyanate esters are primarily determined by the nature of impurities.

In the case of dicyanates, the substitution of Si for C in the bridge linking the aryl cyanate groups in fully cyclotrimerized networks results in a significant decline in the glass transition temperature (from ca. 320 to 260 °C for BADCy and SiMCy, respectively, see Supporting Information Section S4). As a result, the ability to utilize SiMCy for very high

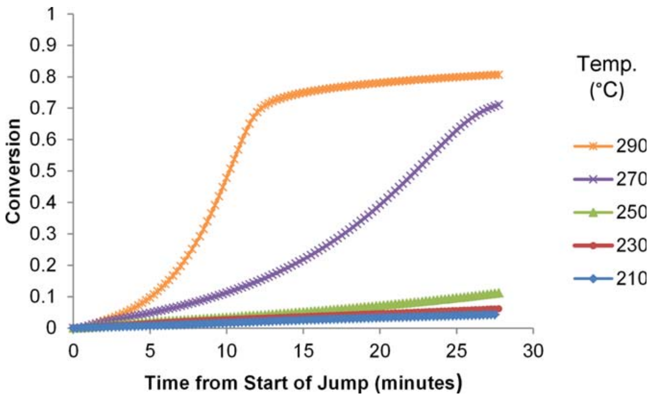

FIGURE 6 Isothermal cure kinetics of SiCy-3 (**3**) after purification by flash chromatography. [Color figure can be viewed in the online issue, which is available at wileyonlinelibrary.com.]

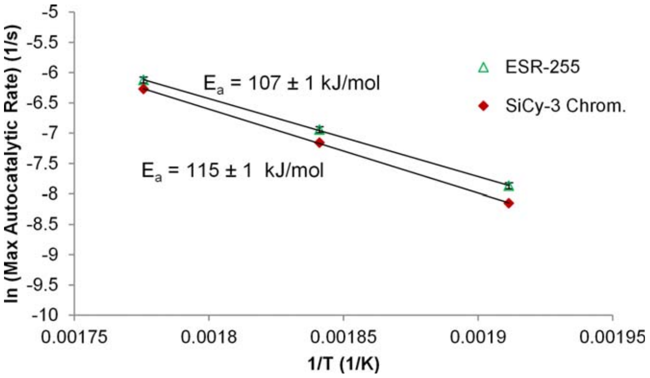

FIGURE 7 Arrhenius plot showing maximum autocatalytic reaction rates of SiCy-3 (**3**, purified by chromatography) and ESR-255. [Color figure can be viewed in the online issue, which is available at wileyonlinelibrary.com.]

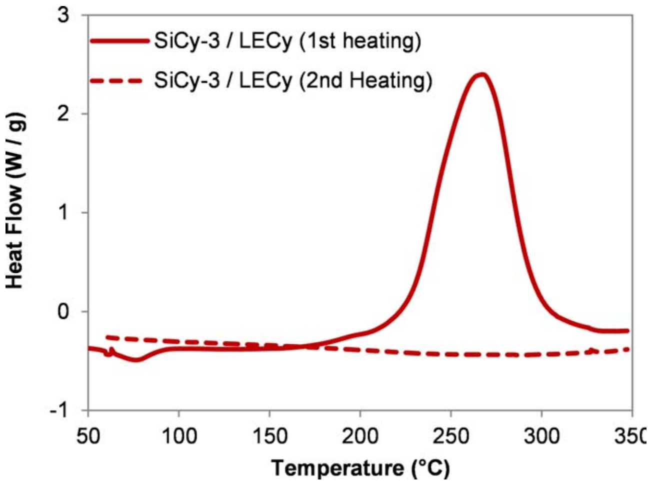

FIGURE 8 Nonisothermal DSC of SiCy-3 (**3**) cocured with an equal weight of LECy. [Color figure can be viewed in the online issue, which is available at wileyonlinelibrary.com.]

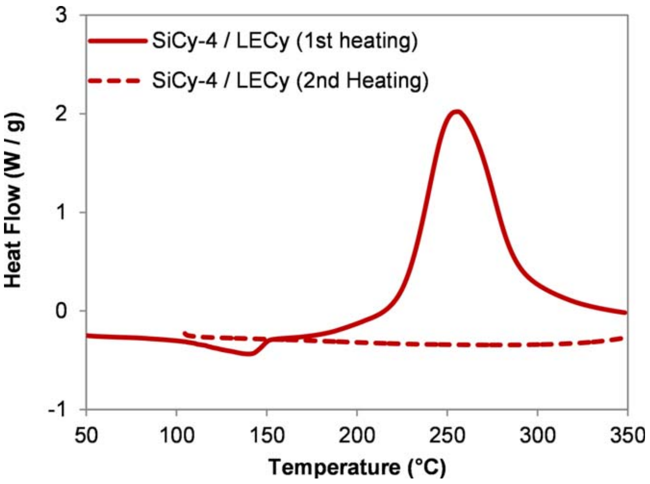

FIGURE 9 Nonisothermal DSC of SiCy-4 (**6**) cocured with an equal weight of LECy. [Color figure can be viewed in the online issue, which is available at wileyonlinelibrary.com.]

temperature applications is more limited compared to BADCy. For the corresponding tricyanates, however, the mechanical softening points of sufficiently cyclotrimerized networks are so high that they are not a factor in limiting high temperature service, and thus substitution of more flexible Si—C bonds for C—C bonds in the bridges connecting aryl cyanates does not adversely affect service temperatures. However, the tricyanate architecture studied comes with the significant drawback of an inability to achieve complete cyclotrimerization due to steric hindrance, which typically leads to decreased thermal and hydrolytic stability in cyanurate networks.

One way to overcome the aforementioned limitation is to cocure monomers such as SiCy-3 with other cyanate esters that can fully cyclotrimerize. Primaset® LECy, a low-viscosity liquid at room temperature featuring a more flexible ethylidene bridge between two aryl cyanates, has long been recognized as an excellent choice for formulating multicomponent cyanate ester mixtures,[85] though formulation with other liquid dicyanates, such as RTX-366,[86,87] is also possible. We investigated the cocuring of SiCy-3 and its tetracyanate analog SiCy-4 with LECy. Figures 8 and 9 show nonisothermal DSC scans of SiCy-3 and SiCy-4, respectively, cocured with an equal weight of LECy. (For these preliminary investigations, purification by chromatography was not attempted.)

The scans show clearly that the crystallization of the tricyanate or tetracyanate component is greatly curtailed, and the melting points lowered, by mixing with LECy. In addition, the cyclotrimerization exotherms are more symmetric, particularly for the SiCy-3/LECy mixture, indicating more complete cyclotrimerization. The enthalpies of cyclotrimerization were 128 ± 13 and 113 ± 11 kJ equiv^{-1} for the SiCy-3 and SiCy-4 mixtures, respectively, indicative of complete cyclotrimerization. Additional evidence for dramatic improvements in the ability to fully cyclotrimerize the mixtures is presented in Figure 10, which shows the FTIR spectra of cured SiCy-3 and cocured SiCy-3/LECy (mixed in equal weights) after 24 h at 210 °C. Peaks near 2250 cm^{-1} due to residual unreacted cyanate ester groups are still clearly present in the neat SiCy-3 network, while in the cocured system the same peaks are almost completely absent. The conversion to cyanurate is confirmed by the presence of the peaks near 1365 and 1550 cm^{-1}.

Physical Properties of Cured Networks

As mentioned previously, the absence of a discernible glass transition in DSC scans of SiCy-3 and SiCy-4 (and their mixtures with LECy), suggests that a glass transition temperature in excess of 350 °C is possible for sufficiently cyclotrimerized networks. Previous studies of cyanate esters have shown that when such high glass transition temperatures are possible, the actual glass transition temperatures obtained during cure are primarily controlled by the cure temperature rather than the glass transition temperature of the fully cured network.[80] This principle is illustrated in Figure 11, which compares DSC traces of BADCy, SiMCy, ESR-

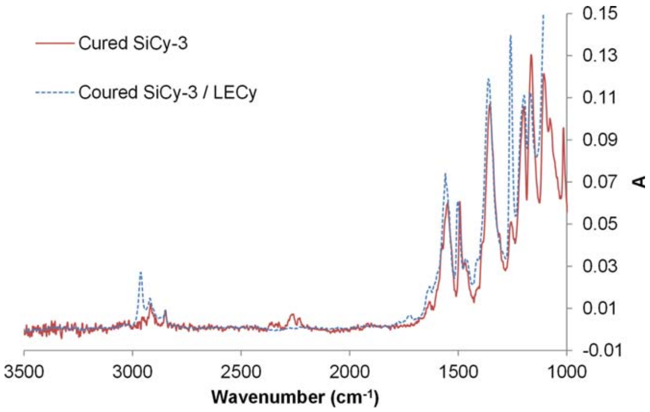

FIGURE 10 FTIR spectra of SiCy-3 (**3**) and a mixture of equal parts SiCy-3 and LECy, after cure for 24 h at 210 °C. [Color figure can be viewed in the online issue, which is available at wileyonlinelibrary.com.]

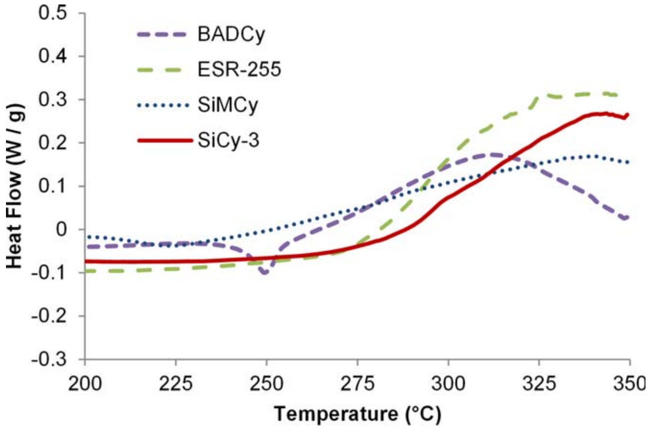

FIGURE 11 DSC scans after cure for 12 h at 210 °C of SiCy-3 (**3**) compared to its carbon-containing analog ESR-255, and the respective silicon- and carbon-containing dicyanate analogs SiMCy and BADCy. The onset of residual cure at around 275–280 °C provides an indication of the T_G after the 12 h cure for the tricyanates, while for the dicyanates, a step change in heat capacity (combined with an endothermic event for BADCy) indicates the T_G. [Color figure can be viewed in the online issue, which is available at wileyonlinelibrary.com.]

255, and SiCy-3 upon quenching and reheating after 12 h at 210 °C in the DSC. For the dicyanates, the step change in heat capacity associated with the glass transition is clearly visible, and occurs between the cure temperature of 210 °C and the glass transition temperature at full cure, which is roughly 260 °C for SiMCy and 320 °C for BADCy. The difference in the "as cured" glass transition temperatures, which were 213 °C for SiMCy and 247 °C for BADCy, principally reflect the difference in the glass transition temperatures of the fully cured networks. In contrast, for both ESR-255 and SiCy-3, the "as cured" glass transition temperatures are between 275 and 280 °C, and are indicated by the onset of significant residual cure (as a result of devitrification) with the step change in heat capacity masked by the cure exotherm. The SiCy-3 appears to have a slightly higher devitrification temperature, which may simply reflect overall faster cure kinetics during the isothermal stage compared to ESR-255. Supporting Information Figures S26 and S27 illustrate the approximate cure kinetics of ESR-255 and SiCy-3 during isothermal cure at 210 °C for 12 h, as gleaned from isothermal DSC data. These data show that SiCy-3 reaches the vitrification point in about 2 h, allowing for 10 h of cure in the glassy state, whereas ESR-255 vitrifies after about 4.5 h, allowing only 7.5 h of cure in the glassy state. We speculate that the longer time available for SiCy-3 to cure in the glassy state may enable SiCy-3 to undergo more cyclotrimerization in the glassy state, which in turn may enable the glass transition in SiCy-3 to climb to a slightly higher temperature.

Analysis of the SiCy-3, SiCy-3/LECy, and SiCy-4/LECy networks was also undertaken by TMA (see Table 1 and Supporting Information Section S5). The TMA scans confirmed that all three networks exhibited glass transition temperatures of at least 360 °C after heating to 350 °C. Thus, for the networks formed by cocuring with LECy, both full conversion and a very high glass transition temperature are possible, making these networks good candidates for dry high-temperature applications. Analysis of moisture uptake, however, revealed a significant weakness. The water uptake of the SiCy-3 network was 5.5%, while that of the SiCy-3/LECy and SiCy-4/LECy networks were 4.7 and 4.4%, respectively, after 96 h immersion at 85 °C of networks cured for 24 h at 210 °C). These values are significantly higher than either ESR-255 (3.5%) or ESR-255 cocured with an equal weight of LECy (2.7%). In order to determine the extent to which sample purity played a role in these results, the same water uptake test was performed on a sample of SiCy-3 further purified by chromatography. The resultant water uptake of 5.0% represents only a modest improvement, and is still much higher than the corresponding value for ESR-255. This result contrasts with earlier results for dicyanates[19] (confirmed by us in catalyzed networks)[17] that show significantly lower water uptake for SiMCy compared to BADCy under identical conditions.

In the dicyanate case, the lower glass transition temperature of SiMCy compared to BADCy is believed to be the key factor that drives the difference in water uptake. The lower glass transition temperature of SiMCy allows for greater relaxation of the free volume formed by cyclotrimerization during cure in the vitreous state, and thereby limits the capacity for water uptake. In fact, when cured at 250 °C (very close to the glass transition temperature for fully cured SiMCy but not for fully cured BADCy), networks of uncatalyzed SiMCy showed half the water uptake compared to networks of BADCy.[19] When catalyzed networks were cured at 210 °C (well below the glass transition temperature for both networks), the water uptake of SiMCy was only about 15% lower than that of BADCy.[17] Because the water uptake values of fully cured cyanurate networks are typically quite similar whether catalyzed or not, the relaxation of free volume near the glass transition temperature appears to be the key factor. As mentioned earlier, the glass transition temperatures achieved by cure at 210 °C were slightly higher for SiCy-3 than for ESR-255, but both were much higher than the cure temperature. ESR-255, however, spent less time in the vitreous state, and may have undergone a lesser extent of cyclotrimerization after

TABLE 1 Key Thermomechanical Properties of Networks Containing SiCy-3 (**3**) and SiCy-4 (**6**) Cured for 24 h at 210 °C

Network[a]	Density (g cc^{-1})	"Fully Cured" T_G (by TMA, °C)	Water Uptake (wt %)	"Wet" T_G (by TMA, °C)
SiCy-3	1.245	>360	5.5	202
SiCy-3/LECy (50/50 wt %)	1.226	>360	4.4	226
SiCy-4/LECy (50/50 wt %)	1.258	>360	4.7	247

[a] Density, water uptake, and "wet" T_G are for networks after 24 h of cure at 210 °C.

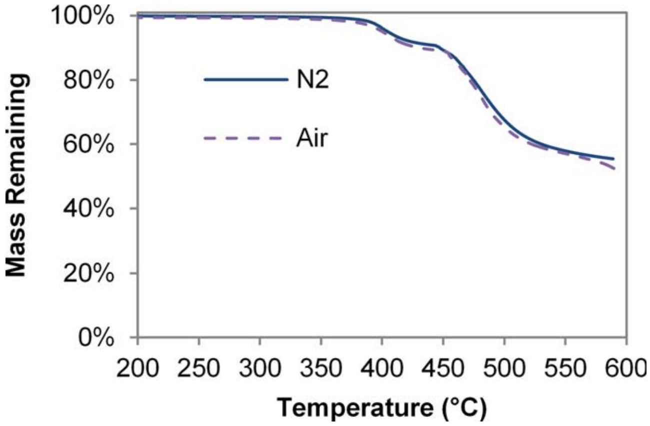

FIGURE 12 TGA traces of cured SiCy-3 (**3**) in nitrogen and air. [Color figure can be viewed in the online issue, which is available at wileyonlinelibrary.com.]

vitrification. These factors suggest the water uptake for the SiCy-3 networks should be higher than for ESR-255. Although the development of free volume during cure in the vitreous state may play an important role in determining the differences in water uptake[88] between networks containing SiCy-3 and ESR-255, a more detailed investigation would be needed to establish the cause with certainty.

As expected the higher water uptake for SiCy-3 and SiCy-3/LECy networks leads to lower "wet" glass transition temperatures (202 and 226 °C, respectively) compared to their ESR-255 analogs (224 and 242 °C, respectively). The SiCy-4/LECy network, however, equals the performance of the ESR-255/LECy network, with a "wet" glass transition temperature (T_G) of 247 °C. The higher water uptake for the silicon-containing networks is expected to lead to faster hydrolytic degradation of the cyanurate networks. The unexpectedly high value of the "wet" T_G for the SiCy-4/LECy network, however, is presently unexplained. It suggests that further exploration of the relationship between network functionality and moisture resistance in cyanurate networks could provide valuable insights that would enhance performance.

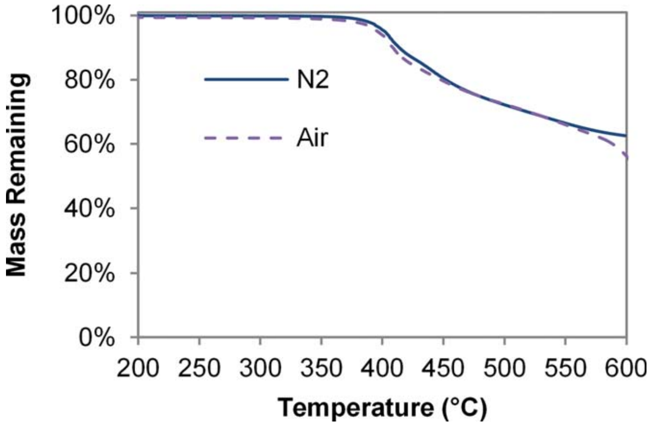

FIGURE 13 TGA traces of cured SiCy-3 (**3**)/LECy (mixed in equal parts by weight before cure) in nitrogen and air. [Color figure can be viewed in the online issue, which is available at wileyonlinelibrary.com.]

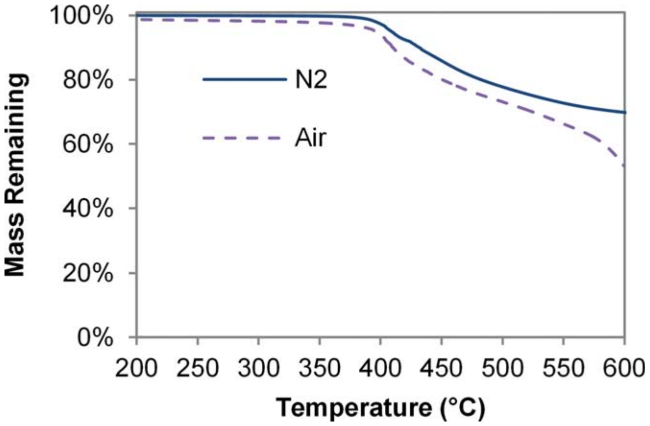

FIGURE 14 TGA traces of cured SiCy-4 (**6**)/LECy (mixed in equal parts by weight before cure) in nitrogen and air. [Color figure can be viewed in the online issue, which is available at wileyonlinelibrary.com.]

A final consideration is the thermochemical stability of the networks. In the dicyanate case, incorporation of Si into the network chains appeared to provide significant protection from oxidation at high temperatures, raising char yields in air to around 50%. As seen in Figures 12–14, TGA traces in nitrogen and air for SiCy-3, SiCy-3/LECy (equal parts by weight), and SiCy-4/LECy (equal parts by weight) networks, respectively, also show char yields in excess of 50% in both nitrogen and air, with the SiCy-4/LECy network providing the best char yield in nitrogen (70%) and similar char yields between 50 and 56% in air for all three networks. A full tabulation of all comparative data (along with graphical data for the ESR-255/LECy networks) is provided in Supporting Information Section S6. Interestingly, ESR-255 networks exhibited higher degradation onset temperatures and higher char yields compared to SiCy-3 networks, while the SiCy-3/LECy networks showed lower degradation onset temperatures but higher char yields than the ESR-255/LECy networks. It is important to note, however, that many factors, such as interactions among network components in multicomponent networks,[85] as well as the extent of cure at the onset of degradation, can affect the thermal decomposition process, so caution is needed when attempting to attribute changes in thermal degradation to changes in the chemical structure of networks.

Nonetheless, taken together, these results indicate that in cases where there is a large difference in the thermochemical degradation of a network in air as compared to nitrogen, the presence of Si appears to provide a consistent improvement in char yield in air. The magnitude of the improvement at 600 °C is much larger than can be accounted for simply by the formation of nonvolatile SiO_2 in place of volatile CO_2 with all else being equal whenever Si is substituted for C in the network structure, suggesting a true protective effect.

However, when thermal degradation in air and under nitrogen are very similar, as is the case for many cyanurate networks with high char yields, then the presence of Si does not improve char yield significantly. Thus, the protective effect appears to be important only if oxidation provides a significant contribution to thermal degradation. Another important point to note is that, in comparison to cyanurate networks in which Si offers a significant protective effect, even higher char yields in air are readily obtained in cyanurate networks with no Si simply by avoiding functional groups (such as isopropylidene bridges between phenyl rings) that promote degradation.[80]

CONCLUSIONS

The synthesis of two new cyanate ester monomers, methyl[tris(4-cyanatophenyl)]silane and tetrakis(4-cyanatophenyl)silane, was achieved in overall yields of around 50% with good purity using a straightforward extension of a three-step method originally developed for the synthesis of bis(4-cyanatophenyl)dimethylsilane from dimethyldichlorosilane. The primary advantage of the new trifunctional and tetrafunctional cyanate ester monomers was the ability to achieve much higher glass transition temperatures (at least 350 °C) at the maximum practical extent of cure. As single-component networks, however, both monomers could not be completely converted to cyanurates due to steric hindrance of the uncured cyanate ester groups. Cocuring with an equal weight of the dicyanate monomer Primaset® LECy, however, enabled practically complete conversion while maintaining a glass transition temperature in the fully cured state of over 350 °C. The higher melting points of the monomers, however, did limit the available processing window, to a modest extent for the neat trifunctional monomer (melting point 118 °C), and severely for the tetrafunctional monomer (melting point 169 °C). Cocured systems, however, retained the favorable processing characteristics of di(cyanate ester) monomers. As with networks formed from di(cyanate ester) monomers, a significant improvement in thermooxidative stability compared to carbon-containing analogs was achieved for silicon-containing networks, but only in cases where oxidation contributed significantly to the thermal degradation. The water uptake for the silicon-containing networks was, in all cases, significantly higher compared to carbon-containing analogs, perhaps due to differences in the evolution of free volume during cure. The higher water uptake leads to a lower "wet" T_G in the silicon-containing networks when compared to their carbon-containing analogs. Nonetheless, the "wet" T_G, at 247 °C, of the best performing networks, produced by cocuring the tetrakis(cyanate ester)-silane with Primaset® LECy, represents outstanding "wet" performance in an easily processed thermosetting resin.

ACKNOWLEDGMENTS

Support from the Air Force Office of Scientific Research and the Air Force research Laboratory, Aerospace Systems Directorate is gratefully acknowledged. The ESR-255 was prepared by Matthew Davis at the Naval Air Warfare Center, Weapons Division (China Lake, CA). C. M. Sahagun performed this work as part of the National Research Council's Research Associateship Program.

REFERENCES AND NOTES

1 Chemistry and Technology of Cyanate Ester Resins; I. Hamerton, Ed.; Chapman & Hall: London, **1994**.

2 C. P. R. Nair, D. Mathew, K. N. Ninan, In New Polymerization Techniques and Synthetic Methodologies; A. A. Abe,-C. Albertsson, H. J. Cantow, Eds.; Advances in Polymer Science 155; Springer: New York, **2001**; Chapter 1, pp 1–99.

3 T. Fang, D. A. Shimp, *Prog. Polym. Sci.* **1995**, *20*, 61–118.

4 I. Hamerton, J. N. Hay, *High Perform. Polym.* **1998**, *10*, 163–174.

5 P. Fabian, M. Haynes, H. Babcock, M. Hooker, *IEEE Trans. Appl. Supercond.* **2013**, *23*, No. 7700204.

6 N. A. Munshi, J. K. Walsh, M. W. Hooker, H. K. Babcock, A. H. Haight, S. R. Durso, A. Kawaguchi, P. Hough, *IEEE Trans. Appl. Supercond.* **2013**, *23*, No. 7700104.

7 P. Abramian, F. de Aragon, J. Calero, J. de la Gama, L. Garcia-Tabares, J. L. Gutierrez, M. Karppinen, T. Martinez, E. Rodriguez, I. Rodriguez, L. Sanchez, F. Toral, C. Vazquez, *IEEE Trans. Appl. Supercond.* **2013**, *23*, No. 4101204.

8 H. C. Chen, K. Shivakumar, *CMC-Comput. Mat. Contin.* **2008**, *8*, 33–42.

9 K. N. Shivakumar, H. Chen, G. Holloway, *J. Reinf. Plast. Compos.* **2009**, *28*, 675–689.

10 P. C. Chen, C. W. Bowers, D. A. Content, M. Marzouk, R. C. Romeo, *Opt. Eng.* **2000**, *39*, 2320–2329.

11 P. D. Wienhold, D. F. Persons, *SAMPE J.* **2003**, *39*, 6–17.

12 R. E. Lyon, R. N. Walters, S. Gandhi, *Fire Mater.* **2006**, *30*, 89–106.

13 H. X. Yan, M. M. Zhang, C. Liu, J. P. Zhang, *Polym. Bull.* **2013**, *70*, 2923–2933.

14 Z. Y. Zhang, A. J. Gu, G. Z. Liang, L. Yuan, D. X. Zhuo, *Soft Matter* **2013**, *11*, 346–352.

15 H. Yu, C. J. Shen, M. Z. Tian, J. Qu, Z. G. Wang, *Macromolecules* **2012**, *45*, 5140–5150.

16 J. T. Reams, A. J. Guenthner, K. R. Lamison, V. Vij, L. M. Lubin, J. M. Mabry, *ACS Appl. Mater. Interfaces* **2012**, *4*, 527–535.

17 A. J. Guenthner, K. R. Lamison, V. Vij, J. T. Reams, G. R. Yandek, J. M. Mabry, *Macromolecules* **2012**, *45*, 211–220.

18 D. X. Zhuo, A. J. Gu, G. Z. Liang, J. T. Hu, L. Cao, L. Yuan, *Polym. Degrad. Stab.* **2011**, *96*, 505–514.

19 A. J. Guenthner, G. R. Yandek, M. E. Wright, B. J. Petteys, R. Quintana, D. Connor, R. D. Gilardi, D. Marchant, *Macromolecules* **2006**, *39*, 6046–6053.

20 M. E. Wright, *Polym. Prepr. (Am. Chem. Soc. Div. Polym. Chem.)* **2004**, *45* (2), 294.

21 E. M. Maya, A. W. Snow, L. J. Buckley, *Macromolecules* **2002**, *35*, 460–466.

22 R. J. Zaldivar, J. Salfity, G. Steckel, B. Morgan, D. Patel, J. P. Nokes, H. I. Kim, *J. Compos. Mater.* **2012**, *46*, 1925–1936.

23 S. K. Dai, A. J. Gu, G. Z. Liang, L. Yuan, *Polym. Adv. Technol.* **2011**, *22*, 262–269.

24 S. K. Pollack, Z. Fu, *Polym. Prepr. (Am. Chem. Soc. Div. Polym. Chem.)* **1998**, *39*, 452–453.

25 S. Devaraju, M. R. Vengatesan, M. Selvi, J. K. Song, M. Alagar, *Microporous Mesoporous Mater.* **2013**, *179*, 157–164.

26 G. L. Wu, K. C. Kou, M. Chao, L. H. Zhuo, J. Q. Zhang, *J. Wuhan Univ. Technol.-Mat. Sci. Edit.* **2013**, *28*, 261–264.

27 W. X. Sun, W. Z. Sun, M. R. Kessler, N. Bowler, K. W. Dennis, R. W. McCallum, Q. Li, X. L. Tan, *ACS Appl. Mater. Interfaces* **2013**, *5*, 1636–1642.

28 E. A. Taha, J. T. Wu, K. Gao, L. Guo, *Chin. J. Polym. Sci.* **2012**, *30*, 530–536.

29 J. T. Hu, A. J. Gu, G. Z. Liang, D. X. Zhuo, L. Yuan, *Polym. Adv. Technol.* **2012**, *23*, 454–462.

30 X. Sheng, M. Akinc, M. R. Kessler, *Polym. Eng. Sci.* **2010**, *50*, 1075–1084.

31 Q. L. Zhang, X. Y. Ma, G. Z. Liang, X. H. Qu, Y. Huang, S. H. Wang, K. C. Kou, *J. Polym. Sci. Part B: Polym. Phys.* **2008**, *46*, 1243–1251.

32 W. K. Goertzen, X. Sheng, M. Akinc, M. R. Kessler, *Polym. Eng. Sci.* **2008**, *48*, 875–883.

33 W. K. Goertzen, M. R. Kessler, *Compos. Part A* **2008**, *39*, 761–768.

34 T. J. Wooster, S. Abrol, D. R. MacFarlane, *Macromol. Mater. Eng.* **2005**, *290*, 961–969.

35 Y. Lin, M. Song, C. A. Stone, S. J. Shaw, *Thermochim. Acta* **2013**, *552*, 77–86.

36 L. Yuan, A. J. Gu, G. Z. Liang, X. Y. Ma, C. Lin, F. Chen, *Polym. Eng. Sci.* **2012**, *52*, 2443–2453.

37 B. John, C. P. R. Nair, K. N. Ninan, *Mater. Sci. Eng. A* **2010**, *527*, 5435–5443.

38 D. A. Kissounko, J. M. Deitzel, S. P. Doherty, A. Shah, J. W. Gillespie, *Eur. Polym. J.* **2008**, *44*, 2807–2819.

39 S. Nagendiran, C. K. Chozhan, M. Alagar, I. Hamerton, *High Perform. Polym.* **2008**, *20*, 323–347.

40 G. I. Anthoulis, E. Kontou, A. Fainleib, I. Bei, Y. Gomza, *J. Polym. Sci. Part B: Polym. Phys.* **2008**, *46*, 1036–1049.

41 V. A. Bershtein, A. M. Fainleib, P. Pissis, I. M. Bei, F. Dalmas, L. M. Egorova, Y. P. Gomza, S. Kripotou, P. Maroulos, P. N. Yakushev, *J. Macromol. Sci. Part B: Phys.* **2008**, *47*, 555–575.

42 Z. P. Fang, H. H. Shi, A. J. Gu, Y. Feng, *J. Mater. Sci.* **2007**, *42*, 4603–4608.

43 D. H. Yu, B. Wang, Y. Feng, Z. P. Fang, *J. Appl. Polym. Sci.* **2006**, *102*, 1509–1515.

44 I. Mondragon, L. Solar, A. Nohales, C. I. Vallo, C. M. Gomez, *Polymer* **2006**, *47*, 3401–3409.

45 T. J. Wooster, S. Abrol, D. R. MacFarlane, *Polymer* **2005**, *46*, 8011–8017.

46 T. J. Wooster, S. Abrol, D. R. MacFarlane, *Polymer* **2004**, *45*, 7845–7852.

47 S. Ganguli, D. Dean, K. Jordan, G. Price, R. Vaia, *Polymer* **2003**, *44*, 6901–6911.

48 S. Devaraju, M. R. Vengatesan, M. Selvi, A. A. Kumar, I. Hamerton, J. S. Go, M. Alagar, *RSC Adv.* **2013**, *3*, 12915–12921.

49 D. X. Zhuo, A. J. Gu, Y. Z. Wang, G. Z. Liang, J. T. Hu, L. Yuan, W. Yao, *Polym. Adv. Technol.* **2012**, *23*, 1121–1128.

50 G. Z. Zhan, X. L. Tang, Y. F. Yu, S. J. Li, *Polym. Eng. Sci.* **2011**, *51*, 426–433.

51 S. Jothibasu, A. A. Kumar, M. Alagar, *High Perform. Polym.* **2011**, *23*, 11–21.

52 Y. Z. Pan, Y. Xu, L. An, H. B. Lu, Y. L. Yang, W. Chen, S. Nutt, *Macromolecules* **2008**, *41*, 9245–9258.

53 R. H. Lin, C. W. Lin, A. C. Lee, Y. H. Chen, F. S. Yen, *J. Appl. Polym. Sci.* **2007**, *103*, 1356–1366.

54 Z. P. Zhang, G. Z. Liang, X. L. Wang, S. Adhikari, J. Z. Pei, *High Perform. Polym.* **2013**, *25*, 427–435.

55 S. Rakesh, C. P. S. Dharan, M. Selladurai, V. Sudha, P. R. Sundararajan, M. Sarojadevi, *High Perform. Polym.* **2013**, *25*, 87–96.

56 S. Jothibasu, S. Devaraju, M. R. Venkatesan, A. Chandramohan, A. A. Kumar, M. Alagar, *High Perform. Polym.* **2012**, *24*, 379–388.

57 A. Chandramohan, K. Dinkaran, A. A. Kumar, M. Alagar, *High Perform. Polym.* **2012**, *24*, 405–417.

58 J. T. Hu, A. J. Gu, Z. J. Jiang, G. Z. Liang, D. X. Zhuo, L. Yuan, B. J. Zhang, X. X. Chen, *Polym. Adv. Technol.* **2012**, *23*, 1219–1228.

59 Z. P. Zhang, J. Z. Pei, G. Z. Liang, L. Yuan, *J. Appl. Polym. Sci.* **2011**, *121*, 1004–1012.

60 Y. Lin, J. Jin, M. Song, S. J. Shaw, C. A. Stone, *Polymer* **2011**, *52*, 1716–1724.

61 K. Liang, H. Toghiani, C. U. Pittman, *J. Inorg. Organomet. Polym. Mater.* **2011**, *21*, 128–142.

62 M. E. Wright, B. J. Petteys, A. J. Guenthner, G. R. Yandek, L. C. Baldwin, C. Jones, M. J. Roberts, *Macromolecules* **2007**, *40*, 3891–3894.

63 K. W. Liang, G. Z. Li, H. Toghiani, J. H. Koo, C. U. Pittman, *Chem. Mater.* **2006**, *18*, 301–312.

64 T. L. Lu, G. Z. Liang, Z. Guo, *J. Appl. Polym. Sci.* **2006**, *101*, 3652–3658.

65 M. E. Wright, B. J. Petteys, A. J. Guenthner, S. Fallis, G. R. Yandek, S. J. Tomczak, T. K. Minton, A. Brunsvold, *Macromolecules* **2006**, *39*, 4710–4718.

66 S. W. Duo, M. M. Song, T. Z. Liu, C. Y. Hu, M. S. Li, *J. Nanosci. Nanotechnol.* **2013**, *13*, 1356–1359.

67 T. K. Minton, M. E. Wright, S. J. Tomczak, S. A. Marquez, L. H. Shen, A. L. Brunsvold, R. Cooper, J. M. Zhang, V. Vij, A. J. Guenthner, B. J. Petteys, *ACS Appl. Mater. Interfaces* **2012**, *4*, 492–502.

68 X. W. Zhang, H. Y. Ren, J. H. Wang, Y. Zhang, Y. Y. Shao, *Mater. Lett.* **2011**, *65*, 821–824.

69 X. E. Cheng, W. F. Shi, *J. Therm. Anal. Calorim.* **2011**, *103*, 303–310.

70 G. H. Hsiue, W. J. Wang, F. C. Chang, *J. Appl. Polym. Sci.* **1999**, *73*, 1231–1238.

71 S. J. Park, F. L. Jin, J. R. Lee, *Macromol. Res.* **2005**, *13*, 8–13.

72 V. Thulasiraman, M. Sarojadevi, *High Perform. Polym.* **2009**, *21*, 437–454.

73 W. J. Wang, L. H. Perng, G. H. Hsiue, F. C. Chang, *Polymer* **2000**, *41*, 6113–6122.

74 Y. L. Liu, C. W. Hsu, C. I. Chou, *J. Polym. Sci. Part A: Polym. Chem.* **2007**, *45*, 1007–1015.

75 C. Y. Chiang, R. S. Tsai, W. J. Shu, *e-Polymer* **2007**, *7*, 1499–1512.

76 H. Y. Tang, N. H. Song, X. F. Chen, X. H. Fan, Q. F. Zhou, *J. Appl. Polym. Sci.* **2008**, *109*, 190–199.

77 R. S. Tsai, Z. Y. Wang, W. J. Shu, *Int. Polym. Proc.* **2010**, *25*, 125–131.

78 A. J. Guenthner, M. C. Davis, K. R. Lamison, G. R. Yandek, L. R. Cambrea, T. J. Groshens, L. C. Baldwin, J. M. Mabry, *Polymer* **2011**, *52*, 3933–3942.

79 D. A. Shimp, S. J. Ising, J. R. Christenson, High Temperature Polymers and Their Uses; Society of Plastics Engineers: Cleveland, OH, **1989**; pp 127–140.

80 A. J. Guenthner, M. C. Davis, M. D. Ford, J. T. Reams, T. J. Groshens, L. C. Baldwin, L. M. Lubin, J. M. Mabry, *Macromolecules* **2012**, *45*, 9707–9718.

81 A. J. Guenthner, G. R. Yandek, J. M. Mabry, K. R. Lamison, V. Vij, M. C. Davis, L. R. Cambrea, Insights into moisture uptake and processability from new cyanate ester monomer and blend studies. SAMPE International Technical Conference; SAMPE International Business Office: Covina, CA, **2010**; paper 42ISTC-119.

82 M. R. Kamal, S. Sourour, *Polym. Eng. Sci.* **1973**, *13*, 59–64.

83 J. M. Kenny, *J. Appl. Polym. Sci.* **1994**, *51*, 761–764.

84 J. T. Reams, Ph.D. Dissertation, South Dakota School of Mines, Rapid City, SD, **2011**.

85 A. J. Guenthner, J. T. Reams, K. R. Lamison, S. M. Ramirez, D. D. Swanson, G. R. Yandek, C. M. Sahagun, M. C. Davis, J. M. Mabry, *ACS Appl. Mater. Interfaces* **2013**, *5*, 8772–8783.

86 S. L. Simon, J. K. Gillham, *J. Appl. Polym. Sci.* **1993**, *47*, 461–485.

87 D. A. Shimp, S. J. Ising, Advanced Materials: the Challenge for the Next Decade. In 35th International SAMPE Symposium and Exhibition; G. Janicki, V. Bailey, H. Schjelderup, Eds.; SAMPE International Business Office, Covina, CA, **1990**; p 1045.

88 O. Georjon, J. Galy, *Polymer* **1998**, *39*, 339–345.